Article:
Pokhrel, B, Chen, Y and Biro, JJ (2019) CFP-1 interacts with HDAC1/2 complexes in C. elegans development. The FEBS Journal, 286 (13). pp. 2490-2504. ISSN 1742-464X

https://doi.org/10.1111/febs.14833

This is the accepted version of the following article: Pokhrel, B., Chen, Y. & Biro, J. J. (2019) CFP-1 interacts with HDAC1/2 complexes in C. elegans development, The FEBS journal, which has been published in final form at https://doi.org/10.1111/febs.14833.

CFP-1 interacts with HDAC1/2 complexes in C. elegans development

Bharat Pokhrel *

bsbp@leeds.ac.uk

School of Molecular and Cellular Biology, Faculty of Biological Sciences,

University of Leeds,

LS2 9JT, Leeds, United Kingdom

Yannic Chen

bsyc@leeds.ac.uk

School of Molecular and Cellular Biology, Faculty of Biological Sciences,

University of Leeds,

LS2 9JT, Leeds, United Kingdom

Jonathan Joseph Biro

jonnybiro@googlemail.com

School of Molecular and Cellular Biology, Faculty of Biological Sciences,

University of Leeds,

LS2 9JT, Leeds, United Kingdom

*Correspondence: bsbp@leeds.ac.uk

Phone: +441133430207

Abstract

CFP-1 (CXXC finger binding protein 1) is an evolutionarily conserved protein that binds to non-methylated CpG-rich promoters in humans and C. elegans. This conserved epigenetic regulator is a part of the COMPASS complex that contains the H3K4me3 methyltransferase SET1 in mammals and SET-2 in C. elegans. Previous studies have indicated the importance of cfp-1 in embryonic stem cell differentiation and cell fate specification. However, neither the function nor the mechanism of action of cfp-1 is well understood at the organismal level. Here we have used cfp-1(tm6369) and set-2(bn129) C. elegans mutants to investigate the function of CFP-1 in gene induction and development. We have characterised C. elegans COMPASS mutants cfp-1(tm6369) and set-2(bn129) and found that both cfp-1 and set-2 play an important role in the regulation of fertility and development of the organism. Furthermore, we found that both cfp-1 and set-2 are required for H3K4 trimethylation and play a repressive role in the expression of heat shock and salt-inducible genes. Interestingly, we found that cfp-1 but not set-2 genetically interacts with Histone Deacetylase (HDAC1/2) complexes to regulate fertility, suggesting a function of CFP-1 outside of the COMPASS complex. Additionally, we found that cfp-1 and set-2 independently regulate fertility and development of the organism. Our results suggest that CFP-1 genetically interacts with HDAC1/2 complexes to regulate fertility, independent of its function within the COMPASS complex. We propose that CFP-1 could cooperate with the COMPASS complex and/or HDAC1/2 in a context-dependent manner.

Keywords: H3K4me3, cfp-1, set-2, Set1/COMPASS complex and HDACs

Introduction

Chromatin regulation shapes gene activity, which underlies many biological processes including development. Histone modifications are a major form of chromatin modification that play a central role in controlling gene expression [1]. The perturbation of these modifications has been associated with developmental defects and diseases including cancer [2-4]. However, the mechanism by which histone modifications contribute to these events is yet to be fully determined.

The interplay between the highly dynamic histone modifications can determine chromatin regulation and gene function [5]. At enhancer and promoter regions histones are subjected to high turn-over of acetylation or methylation modifications which results in either activation or repression of gene expression [6-8]. Acetylation of histones by conserved histone acetyltransferases (HATs) such as Gcn5, p300/CBP, sRC/p160 and MYST is related to gene expression. Whereas deacetylation of histone by evolutionarily conserved histone deacetylases (HDACs) is often associated with gene repression [7, 9, 10]. HDACs form multiprotein complexes such as SIN3, NuRD, and CoREST complexes to regulate gene expression [7].

One of the most studied chromatin modifications is histone 3 lysine 4 trimethylation (H3K4me3). H3K4me3 is found at 5′ sites of active genes and is often regarded as an active promoter mark [11, 12]. Previous studies have shown that the level of H3K4me3 is strongly correlated with gene expression of a subset of genes. These studies have suggested that H3K4me3 could contribute to gene expression by acting as a binding site for chromatin modifiers and transcriptional machinery to facilitate the transcription process [13-16]. Contrary

to the role of H3K4me3 in gene expression, growing evidence has suggested that H3K4me3 could play a repressive role in gene expression [17-19]. All these findings generated from different organisms suggest that H3K4me3 could play a role in both gene expression and repression in a context-dependent manner. Nevertheless, how H3K4me3 contributes to gene expression and repression needs to be explored further.

H3K4me3 is deposited by a Complex Proteins Associated with Set1 (COMPASS) complex [2]. The COMPASS complex is evolutionarily conserved from yeast to mammals. In yeast, there is only one complex which is responsible for all forms of H3K4 methylation (H3K4me1, H3K4me2, and H3K4me3), whereas in humans there are six COMPASS complexes: SET1A, SET1B and Mixed Lineage Leukemia (MLL) 1, 2, 3 and 4. SET1A and SET1B are responsible for the majority of H3K4me3 mark deposition, MLL 1 and 2 are responsible for H3K4me3 deposition in a subset of genes, and MLL 3 and MLL 4 are responsible for H3K4me1 [2]. In C. elegans there are two COMPASS complexes: SET-2/COMPASS, a direct descendent of yeast Set1, and SET-16/COMPASS which is the MLL 3/4 ortholog [20, 21]. Although Set1 is the key subunit of COMPASS, its associated subunits are also important for assembly and regulation of H3K4 methylation [2, 22].

One of the major subunits of the COMPASS complex is CFP1 which is essential for H3K4me3 modifications [23-25]. CFP1 binds to unmethylated CpG-rich DNA sequences known as CpG islands (CGIs) and helps in the recruitment of the SET1/COMPASS complex at the promoter region of active genes [26-30]. Previous studies have reported that CFP1 plays an important role in cell fate specification and cell differentiation [24, 25, 31]. However, the exact mechanism by which CFP1 contributes to gene regulation and development is not clear. To understand the role of cfp1 in gene regulation and development, we have used cfp-1(tm6369) and set-2(bn129) C. elegans mutants. We discovered that deletion of cfp-1 or set-2 results in

drastic reduction of H3K4me3 levels and stronger expression of heat shock and salt-inducible genes. Surprisingly, we found that despite both genes being essential for H3K4me3 deposition and gene induction, only CFP-1, but not SET-2 genetically interacts with HDAC1/2 in C. elegans development. This study suggests that in addition to the canonical function of CFP-1 in the H3K4me3 deposition, CFP-1 also cooperates with HDAC 1/2 complexes during C. elegans development.

Results

CFP-1 is required for fertility and normal growth rate

In yeast and mammals, COMPASS/Set1 is responsible for the majority of H3K4me3. Loss of SET1 or CFP1 results in drastic reduction of H3K4me3 levels at 5′ sites of active genes [23, 24, 32-34]. Similar to mammals and yeast, the function of set-2 (homolog of SET1) and cfp-1 (homolog of CFP1) in H3K4me3 deposition is also conserved in C. elegans [20, 21, 35]. To further investigate the role of cfp-1 in development, cfp-1(tm6369) mutant was used in this study. cfp-1(tm6369) is a deletion allele, which has 254bp deletion encompassing exon 5 of F52B11.1a.1 and part of the intron upstream and downstream (Fig. 1A). Exon 5 is conserved in all transcripts of the cfp-1 gene, therefore deletion on exon 5 region of F52B11.1a.1 results in truncation in all the transcripts of the cfp-1 gene. To confirm that cfp-1(tm6369) is a loss of function allele we measured the global level of H3K4me3 in both the cfp-1(tm6369) and the set-2(bn129) loss of function mutants by western blot analysis. We observed that the levels of H3K4me3 in cfp-1(tm6369) mutant is significantly reduced and was similar to that reported for the set-2(bn129) allele (Figure 1B) suggesting that the cfp-1(tm6369) mutant is a loss of function allele.

To explore the functional consequences of loss of cfp-1 in C. elegans we pursued the phenotypic characterisation of the cfp-1(tm6369) mutant by conducting a fertility assay and measured the growth rate. For the fertility assay, we measured the brood size of cfp-1(tm6369) and set-2(bn129) mutants at 20 ℃ and 25 ℃. 20 ℃ is an optimum temperature for C. elegans, we observed that at 20 ℃ both mutants had a significant reduction in brood size compared to wild type (Figure 1C). 25 ℃ is known as a non-permissive temperature for C. elegans growth. We observed that at 25 ℃ fertility was severely affected in both cfp-1(tm6369) and set-2(bn129) mutants compared to wild-type (Figure 1D). In a previous study, it was reported that set-2(bn129) mutant display a mortal germline phenotype indicative of a progressive loss of brood size over generations leading to sterility, at 25 ℃ [35]. We also investigated the mortal germline phenotype of the cfp-1(tm6369) mutant at 25 ℃. L4 larvae (P0) maintained at 20 ℃, were transferred to 25 ℃ and the average brood size of F1, F2, F3 and F4 generation at 25 ℃ was measured. Surprisingly, the F2 generation of the cfp-1(tm6369) mutant at 25 ℃ was completely sterile (Figure 1E). Taken together, these findings suggest that both cfp-1 and set-2 play an important role in maintaining fertility.

We measured the growth rate of set-2(bn129) and cfp-1(tm6369) mutants and compared them to wild-type. C. elegans embryos pass through four larval stages (L1, L2, L3 and L4) to reach adulthood. We measured the growth of freshly laid embryos of wild-type, cfp-1(tm6369) and set-2(bn129) mutants at 60 h. Both cfp-1(tm6369) and set-2(bn129) mutants show delays in development from embryo to adult (Figure 1F). After 60 h, ~84% of wildtype embryos reached the adult stage, whereas most of the cfp-1(tm6369) and set-2(bn129) mutants were still in the L4 stage (Figure 1F). These results further evidence that both cfp-1 and set-2 are required for the proper development of an organism.

CFP-1 and SET-2 attenuate gene induction

We next investigated the role of cfp-1 and set-2 in gene expression by using salt-inducible reporter strain VP198 (kbIs5 [gpdh-1p::GFP + rol-6(su1006)]). The VP198 contains green fluorescent protein (GFP) reporter gene downstream of the gpdh-1 gene promoter and is expressed in a higher salt environment (Figure 2A) [36]. We crossed this strain with cfp-1(tm6369) and set-2(bn129) mutants to generate cfp-1(tm6369);kbIs5 and set-2(bn129);kbIs5 double mutant strains and exposed them to a higher salt concentration (150 mM NaCl). C. elegans is normally grown on a salt concentration of 52 mM. Thus 52 mM was used as a control throughout this study.

When exposed to hypertonic stress, we observed that higher percentage of both cfp-1(tm6369);kbIs5 and set-2(bn129);kbIs5 mutants displayed hyper-induction of the reporter gene compared to wild-type worms (Figure 2B). The intensity of expression was also higher in both the mutants compared to wild-type. We also measured the endogenous transcript level of gpdh-1 gene at control and at higher salt concentrations in wild-type, cfp-1(tm6369) and set-2(bn129) mutants. We found that at higher salt concentration, the level of the gpdh-1 transcript was highly induced in cfp-1(tm6369) and set-2(bn129) mutants compared to wild-type (Figure 2C).

To further investigate the role of cfp-1 and set-2 in gene induction regulation, we used the heat shock reporter strain AM722 [rmIs288(hsp70p::mCherry IV)]. AM722 contains mCherry downstream of heat shock promoter hsp-70, which is expressed during heat stress (Figure 2D) [37]. We crossed this strain with cfp-1(tm6369) and set-2(bn129) to generate cfp-1(tm6369);rmIs288 and set-2(bn129);rmIs288 strains. We found that after heat shock, mCherry expression was significantly higher in cfp-1(tm6369);rmIs288 and set-2(bn129);rmIs288 strains compared to rmIs288 in a wild-type background (Figure 2D and E).

We also measured the endogenous expression of heat-inducible genes, C12C8.1, F44E5.4 and hsp-16.2 in the cfp-1(tm6369) and set-2(bn129) mutant backgrounds. C12C8.1, F44E5.4 and hsp-16.2 are heat inducible chaperones downstream of the heat shock factor -1 (hsf-1) gene and are expressed during heat stress [38-40]. After heat shock at 33 ℃ for one hour, the expression of C12C8.1, F44E5.4 and hsp-16.2 were significantly upregulated in both cfp-1(tm6369) and set-2(bn129) mutants compared to wild-type (Figure 2F). Higher induction of heat and salt-inducible genes in both cfp-1(tm6369) and set-2(bn129) mutants with a negligible level of H3K4me3 suggests that H3K4me3 can indeed play a repressive role in gene induction.

CFP-1 cooperates with class I HDACs to regulate fertility

We conducted a mini fertility screen to find the candidate genes that could either enhance or suppress the observed poor fertility phenotype of the cfp-1(tm6369) mutant. Previous studies have illustrated that crosstalk between COMPASS and histone acetylation plays an important role in ensuring proper gene regulation [41-43]. Thus, for the screen, we selected histone acetyltransferases (cbp-1, mys-4 and hat-1) and histone deacetylases (hda-1, hda-2 and hda-3). We either knocked down cbp-1 or hat-1 by RNAi on cfp-1(tm6369) and set-2(bn129) or crossed mys-4(tm3161) mutant with cfp-1(tm6369) or set-2(bn129) mutants and measured the effect on fertility. In the fertility screen, we did not observe any significant change in brood size of cfp-1;mys-4 and set-2;mys-4 double mutants, and during RNAi knockdown of hat-1 in cfp-1(tm6369) and set-2(bn129) mutants (Figure 3A and 3B). cbp-1 RNAi resulted in a larval arrest in wild-type, cfp-1(tm6369) and set-2(bn129) mutants so brood size could not be determined. However, we did not observe significant changes in fertility of the cbp-1(ku258) gain of function mutant during cfp-1 or set-2 RNAi (Figure 3C) [44].

In contrast to HATs, RNAi knockdown of hda-1 or hda-2 or hda-3 in cfp-1(tm6369) mutant

significantly reduced the brood size, suggesting a synergistic genetic interaction between these histone deacetylases and cfp-1 (Figure 3D and 3E). Interestingly, we found that unlike cfp-1(tm6369), set-2(bn129) brood size did not significantly reduce in RNAi of hda-1 or hda-2 or hda-3 (Figure 3D and 3E).

We demonstrated that set-2 and cfp-1 play a similar role in fertility and development of C. elegans. However, we observed that RNAi knockdown of hda-1 or hda-2 or hda-3 only enhances the low brood phenotype of cfp-1(tm6369) mutant. Different responses of the cfp-1(tm6369) and set-2(bn129) mutants to the same RNAi conditions could be due to differential sensitivity to RNAi. To investigate this, we carried out an RNAi sensitivity assay. We measured the RNAi sensitivity of cfp-1(tm6369) and set-2(bn129) mutants using hmr-1, dpy-10 and unc-15 genes with well-defined phenotypes. We found that both cfp-1(tm6369) and set-2(bn129) mutants responded similarly to the tested RNAi (Table 1). This suggests that the different response of cfp-1(tm6369) and set-2(bn129) mutants in hda-1 or hda-2 or hda-3 RNAi background is not due to the different sensitivity to RNAi.

Table 1. **RNAi sensitivity assay:** Sensitivity of wild-type, set-2(bn129) and cfp-1(tm6369) on RNAi was measured using dpy-10, unc-15 and hmr-1 RNAi. dpy-10 was scored based on the severity of dumpy (shorter and fatter body morphology) phenotype. More + means stronger phenotype. unc-15 was scored based on the severity of uncoordinated phenotype (paralysis). More + means stronger phenotype. hmr-1 was scored based on the percentage of dead eggs out of total brood. <6% means that there was less than 6% embryonic lethality in wild-type, set-2(bn129) and cfp-1(tm6369) on hmr-1 RNAi. This experiment has been repeated 2 times, and similar results were observed.

RNAi	Wild-type	cfp-1(tm6369)	set-2(bn129)
EV (Control)	-	-	-
hmr-1	<6%	<6%	<6%
dpy10	+++++	+++++	++++
unc-15	+++++	++++	+++++

CFP-1 interacts genetically with SIN-3, CHD-3 and SPR-1 complexes

hda-1, hda-2 and hda-3 are the orthologs of mammalian class I HDACs (HDAC1/2) [45]. HDAC1/2 are found in multiprotein complexes such as Sin3, NuRD and CoREST which contain Sin3, Mi2-α/β and CoREST as a major subunit, respectively [46-49]. Sin3 acts as a scaffold for the assembly of Sin3/HDAC1/2 complex [50]. CoREST of CoREST/HDAC1/2 complex helps in recognition of nucleosome substrate and stimulates the nucleosome modifying activities of HDAC1/2 [51]. NuRD complex contain either Chromodomain-helicase-DNA-binding proteins, CHD3 (Mi2-α) or CHD4 (Mi2-β) as major subunits. Mi2-α/β are ATPases which use ATP to unwind the nucleosomes [52, 53]. Sin3, CoREST and Mi2-α/β are relatively specific to Sin3, CoREST and NuRD complex respectively and are thought to be defining components of these complexes [50-53].

To test which of these complexes interact with cfp-1, we carried out RNAi knockdown of C. elegans orthologs of SIN3, Mi-2 and CoREST in cfp-1(tm6369) mutant. Interestingly, RNAi knockdown of SIN3 ortholog, sin-3, dramatically reduced the average brood size of cfp-1(tm6369) mutant (Figure 4A). This suggests cfp-1 interacts with sin-3 to regulate fertility. To

243 further confirm the RNAi results, we crossed sin-3(tm1276) mutant with cfp-1(tm6369) mutant
244 and generated the cfp-1(tm6369);sin-3(tm1276) double mutants. We found that all of the cfp-
245 1(tm6369);sin-3(tm1276) double mutants were completely sterile (Figure 4B). Similar to sin-
246 3 RNAi, RNAi mediated knockdown of CoREST ortholog, spr-1, on cfp-1(tm6369) mutant
247 significantly reduced the average brood size (Figure 4A). We also crossed the cfp-1(tm6369)
248 mutant to spr-1(ok2144) and measured the fertility. We observed the stronger reduction in the
249 average brood size of cfp-1(tm6369);spr-1(ok2144) double mutant compared to single mutants.
250 (Figure 4C).

251 C. elegans has two homologs of Mi-2, LET-418 and CHD-3 [54]. Loss of function allele of
252 let-418 has a strong fertility defect and sterility [54-59]. Since we used fertility to study the
253 genetic interaction between genes, it would be difficult to distinguish whether the further
254 reduction (if any) on the brood of cfp-1(tm6369) mutant on let-418 RNAi is due to additive or
255 synergistic effect. Thus, we used chd-3 to study the genetic interaction between NuRD complex
256 and CFP-1. We observed that the average brood size of cfp-1(tm6369) mutant treated on CHD-
257 3 RNAi was significantly reduced compared to control RNAi (Figure 4A). These findings
258 support that cfp-1 interacts with SIN3, NuRD and CoREST complexes.

259 On the other hand, we did not observe the synergistic reduction in the average brood size of
260 set-2(bn129) mutant on sin-3 or chd-3 or spr-1 RNAi (Figure 4A). Additionally, the average
261 brood size of set-2(bn129);spr-1(ok2144) and set-2(bn129);sin-3(tm1276) double mutants
262 was similar to single mutants (Figure 4B and 4C). These results suggest that set-2 does not
263 interact with SIN3, NuRD and CoREST complexes. It is possible that SET-2 and HDAC
264 complex act on the same pathway to regulate fertility. Collectively, these findings support that
265 cfp-1 interacts with HDAC1/2 complexes and the interaction is independent of SET-2.

266 We sought to investigate the functional link between cfp-1 and HDAC1/2 complexes. One of

the main functions of HDAC1/2 complexes is histone deacetylation, so we asked if the inhibition of HDAC1/2 deacetylase enhances the low brood phenotype of cfp-1(tm6369) and set-2(bn129) mutant or not. We treated the cfp-1(tm6369) worms with Trichostatin A (TSA). TSA is a chemical that inhibits class I/II histone deacetylase and TSA treated cells have a significant gain in histone acetylation [60]. TSA is a toxic chemical, thus we used 4 uM which is an established non-toxic dose for C. elegans [61]. We found that the average brood size of wild-type and set-2(bn129) mutant were not affected. In contrast, the brood size of cfp-1(tm6369) mutant was slightly but significantly reduced (Figure 4D). This further confirms the genetic interaction between cfp-1 and HDAC1/2 and provide the functional link between cfp-1 and HDACs.

cfp-1 and set-2 independently regulate fertility and growth

We did not observe any genetic interaction between set-2 and tested HDACs, but we found a clear genetic interaction between cfp-1 and HDAC1/2 complexes. This finding suggested that cfp-1 and set-2 might act in separate pathways to regulate fertility. To investigate this, we generated cfp-1(tm6369);set-2(bn129) double mutant and measured the brood size. If both cfp-1 and set-2 act in a similar pathway, then the average brood size of double mutants should be similar to single mutants. Interestingly, we found that the average brood size of cfp-1(tm6369);set-2(bn129) double mutant was significantly lower than the average brood size of cfp-1(tm6369) and set-2(bn129) single mutants (Figure 5A). This clearly suggests that cfp-1 and set-2 act in separate pathways or even in separate molecular complexes to regulate fertility. We also carried out growth kinetics of cfp-1(tm6369);set-2(bn129) double mutant and compared to cfp-1(tm6369) and set-2(bn129) single mutants. We found that the double mutant grows slower compared to single mutants (Figure 5B). Taken together, these findings suggest

that even though cfp-1 and set-2 are key subunits of COMPASS complex, they act in separate pathways or in separate molecular complexes in C. elegans development.

Discussion

Over the past decade, various research groups have emphasized the importance of CFP-1 in cell fate specification and cell differentiation. However, the contribution of CFP1 to gene regulation is not fully understood. In this study, we set out to elucidate the impact of the loss of CFP-1 on gene induction and development by using cfp-1(tm6369) and set-2(bn129) C. elegans mutants. Phenotypic characterisation of cfp-1(tm6369) and set-2(bn129) mutants suggests that CFP-1 and SET-2 play an important role in fertility and development of C. elegans. We found that in cfp-1(tm6369) and set-2(bn129) mutants, the induction of heat and salt-inducible genes were significantly higher than the wild-type. The similar function of CFP-1 and SET-2 in fertility and in gene induction supports that CFP-1 function in a COMPASS complex. However, we also found that CFP-1 and SET-2 act in separate pathways or possibly on separate molecular complexes to regulate fertility. Furthermore, we found that CFP-1 but not SET-2 genetically interacts with HDAC1/2 complexes to regulate fertility. These findings suggest a function of CFP-1 outside of the Set1/COMPASS complex. We propose that CFP-1 could interact with the COMPASS complex and the HDAC1/2 complexes in a context-dependent manner (Figure 6).

CFP-1 and SET-2 are major subunits of the COMPASS complex responsible for bulk H3K4me3 [20, 21, 35]. Here, we observed that loss of function of CFP-1 or SET-2 results in a dramatic reduction of the H3K4me3 level. We also observed the hyper-induction of salt and heat-inducible genes following the loss of function of CFP-1 or SET-2. The observed hyper-induction could be due to an increase in chromatin accessibility in the loss of H3K4me3. This could be supported by the fact that in yeast H3K4me2/3 repress GAL1 gene induction by recruiting histone deacetylase complex called RPD3S [17]. Recruited RPD3S could promote

chromatin compaction by deacetylation of nearby histones. Similarly, another study suggests that H3K4me3 acts as a memory to repress the GAL1 reactivation by recruiting Isw1 ATPase which limits the RNA polymerase II activity [62]. In this study, it was observed that CFP-1 genetically interacts with HDAC1/2 complexes in C. elegans development. In addition to DNA binding domain, mammalian CFP-1 also contains a PHD domain that binds to H3K4me3 [31, 34]. The PHD finger could also be conserved in C. elegans CFP-1, and CFP-1 may bind to H3K4me3via its PHD domain and helps in the recruitment of the HDAC complex at the promoter region. HDACs recruited to H3K4me3 sites could deacetylate the nearby histone to establish the repressive chromatin state. Thus, restricting the binding of transcription factors such as HSF-1.

Alternatively, CFP-1 and SET-2 may play an important role in maintaining the structure of chromatin and in the loss of CFP-1 or SET-2 results in increase in chromatin accessibility. Therefore, in the loss of function of CFP-1 or SET-2, rate of recruitment of HSF-1 or other TFs could increase. It is also possible that CFP-1 and SET-2 may play a role in the activation of stress-inducible genes such as HSF-1 genes. For example, during heat stress, HSF-1 is activated and translocated into the nucleus. CFP-1 and SET-2 might restrict the nuclear localisation of HSF-1. Thus, in the loss of function of CFP-1 or SET-2, the rate of nuclear translocation of HSF-1 could have increased, leading to increased gene expression. Another plausible explanation for the observed hyper induction in the mutants is that CFP-1 and SET-2 could contribute to gene induction by altering the regulation of RNA polymerase II (Pol II) pausing. Paused Pol II is found in the promoter of hsp genes, and are primed for transcription activation in response to a stimulus [63]. CFP-1 and SET-2 could act as regulators to maintain paused Pol II in the promoter regions and prevent the burst of transcription.

In previous studies, it has been suggested that CFP-1 and SET-2 helps in the maintenance of

germ cell integrity and loss of function of CFP-1 or SET-2 results in increased expression of somatic genes in the germ cells [19, 35, 64]. Furthermore, loss of function of SET-2 or CFP-1 results in a downregulation of genes involved in reproduction and embryonic development [65]. Here we observed significant reduction in the average brood size of the cfp-1(tm6369) and the set-2(bn129) mutants. The observed reduction in the brood size of both the mutants could be due to the downregulation of genes that are required for fertility and reproduction.

Reduced fertility and slow growth phenotype of cfp-1(tm6369) and set-2(bn129) mutants suggest that CFP-1 and SET-2 could act in same pathway to regulate the fertility and development in C. elegans. Surprisingly, we observed that the brood size of the cfp-1(tm6369);set-2(bn129) double mutant was significantly lower than single mutants suggesting that CFP-1 and SET-2 might act in different pathways or in molecular complexes to regulate fertility and development. Additionally, we observed that loss of key subunits of HDAC1/2 complexes resulted in a synergistic reduction of average brood size of the cfp-1(tm6369) mutant but not of set-2(bn129) mutant. Observed synergistic reduction in the brood size of cfp-1(tm6369) mutant upon RNAi of key subunits of HDAC1/2 complexes could be due to misregulation of genes involved in fertility. It is possible that CFP-1 together with SET-2, regulate the expression of some set of genes involved in fertility and development, and CFP-1 together with HDAC1/2 complexes, regulate the other set of genes involved in fertility. Recently, it has been observed that loss of function of SET-2, SIN-3 and CFP-1 results in a downregulation of genes involved in reproduction and embryonic development. Also, some sets of genes are mis-regulated only in cfp-1 and set-2 mutants, and some are only in cfp-1 and sin-3 mutants [65].

In previous studies it has been observed that CFP-1, but not SET-2, can suppress the synthetic multivulva phenotype in C. elegans [21, 64, unpublised data]. Similary, in yeast, it has been

observed that Spp1 (yeast ortholog of cfp-1) exist in the Mer2-Spp1 complex [66]. This suggests that CFP-1 can also exist in other molecular complexes and function independent of SET-2/COMPASS complex. Here we observed that CFP-1 but not SET-2 interacts genetically with HDAC1/2 complexes to regulate fertility. Recently, it has been suggested that CFP-1 is present in Sin-3/HDAC complexes in C. elegans [65]. It is possible that CFP-1 is also present in other HDAC1/2 complexes (CHD-3 and SPR-1).

Similar function of CFP-1 and SET-2 in gene induction and H3K4me3 modification suggest that CFP-1 function within SET-2/COMPASS complex. The observed SET-2 independent interaction of CFP-1 with HDAC1/2 complexes suggests that CFP-1 can exist in HDAC1/2 complexes. Based on these finding, we propose that CFP-1 could interact with Set1/COMPASS and/or HDACs complexes in a context-dependent manner (Figure 6).

Materials and methods

Strains and their Maintenance

The following strains were used for experimental purpose. N2(wild-type), set-2(bn129), cfp-1(tm6369), mys-4(tm3161), set-2(bn129);mys-4(tm3161), cfp-1(tm6369);mys-4(tm3161), cbp-1(ku258), rmIs288, cfp-1(tm6369);rmIs288, set-2(bn129);rmIs288, kbIs5[gpdh-1p::GFP+rol-6(su1006)], cfp-1(tm6369);kbIs5, cfp-1(tm6369);kbIs5, spr-1(ok2144), set-2(bn129);spr-1(ok2144), cfp-1(tm6369);spr-1(ok2144), sin-3(tm1276), set-2(bn129);sin-3(tm1276), and cfp-1(tm6369);sin-3(tm1276). Worms were maintained at 20 °C unless stated at standard growth condition. They were grown on Escherichia coli OP50 seeded Nematode Growth Medium (NGM) petri plates.

Western Blot

Embryos obtained from bleached adult worms were transferred in 15 ml Falcon tubes containing 10 ml of M9 buffer. Tubes were left on a shaker overnight at 20 °C to obtain starved L1 worms. Starved L1 (3.2-3.5 $x10^3$) worms were pelleted in M9 buffer and snap-frozen at −80 °C. Pellets were recovered in lysis buffer (50 mM Tris-Cl (pH 8), 300 mM NaCl, 1 mM PMSF, 1 mM EDTA, 0.5% Triton X-100 and protease inhibitor cocktail (Xiao et al., 2011). These worms were sonicated at 20% amplitude for 5-10 seconds, this step was repeated two times. Lysed samples were centrifuged at 12,000 rpm for 15 minutes at 4 °C, and supernatants were collected. Protein concentration in the supernatant was measured by the Bradford method. These samples were resolved on SDS-PAGE where 50 µg of total protein was loaded in each well. The protein was transferred to the nitrocellulose membrane using BioRed western blot system at 25V, 1 A for 1 h. The membrane was cut into two parts based on the molecular weight of tubulin ~50 kDa, and Histone3 ~15 kDa. Membranes were incubated with 5% non-fat milk in TBST (Tris-buffered saline, 0.1% Tween 20) for 1 h and subsequently incubated overnight at 4 °C with 1:5,000; anti-H3K4me3, 1:5,000; anti-H3 or 1:5,000; anti-tubulin antibodies. The membrane was washed twice with TBST and incubated with 1:5,000 dilutions of HRP-linked secondary antibodies. After incubation with the secondary antibody, the membrane was washed thrice with TBST for 10 min. After the wash step, the membrane was developed by super signal west pico plus chemiluminescent substrate (Thermo Scientific) and imaged using Alliance Q9 advanced gel imager (Uvitec, Cambridge). Since H3 and H3K4me3 were of similar molecular weight, we loaded the same samples (same amount) in two different wells of the same gel. We used one set of samples for H3 detection and another for H3K4me3 detection. H3 and tubulin were used as loading controls. The following antibodies were used for western blot analyses: mouse monoclonal anti H3K4me3 (Wako chemicals), polyclonal rabbit anti-total H3 (Abcam) and mouse monoclonal anti-tubulin (Sigma).

Brood size assay

For brood size at 20 ℃, either ten L4 worms were picked and transferred to an individual plate, or 3-5 L4 larvae per plate were picked onto two to three plates. Worms were transferred onto new plates every day or every other day until laying ceased. Old plates were counted for a total number of eggs and were stored at 20 ℃ for ~24-48 h and subsequently scored for the number of live progeny. Animals that crawl out of the plates and lost were not included (Xiao et al., 2011).

For Brood size at 25 ℃, twenty L4 worms were picked from 20 ℃ and transferred to new OP50 seeded plates. They were allowed to lay eggs for overnight at 25 ℃. Next day, all mother worms were picked and transferred to new plates and left for 5-6 h. Mothers from new plates were removed, and eggs were allowed to reach L4 at 25 ℃. From the new plate, ten L4 worms were picked and transferred to an individual plate. Worms were transferred into new plates every day or every other day until they stop laying. Old plates were counted for a total number of eggs on plates and were stored at 25 ℃ for ~24-48 h and subsequently scored for the number of live progeny. For the Mrt assay, brood size of subsequent generation at 25 ℃ was assayed. Animals that crawled out of the plates and lost were not included.

Student T-tests were performed to investigate the potential interaction between the two genes. Under null hypothesis, where no genetic interaction between two genes is assumed, the expected brood size of the double mutants (or RNAi knockdown of a gene in a single mutant) is the product of the brood size of the single mutants (or single mutant and the RNAi knockdown of the gene in a wild-type) divided by the average brood size of wildtype. A one-

sided T-test is done to compare the expected (under null-hypothesis) brood size with the observed brood size of double mutants (or RNAi knockdown of a gene in a single mutant).

$$Brood_{H_0} = \frac{Brood_{gene\ 1} \times Brood_{gene\ 2}}{Brood_{WT}}$$

$Brood_{H_0}$ = Expected Brood size of double mutant (or RNAi) under the null hypothesis

$Brood_{gene\ 1}$ = Actual Brood size of first mutant (or RNAi)

$Brood_{gene\ 2}$ = Actual Brood size of second mutant (or RNAi)

$Brood_{WT}$ =Actual Brood size of Wild-type

Growth Kinetics assay

Twenty-forty synchronised L4 worms were picked from 20 °C and transferred to new OP50 seeded plates. They were allowed to lay eggs for overnight at 20 °C. Next day, all mother worms were picked and transferred to new plates to lay eggs and left for 5-6 h. Mothers from the new plates were removed, and eggs were left to grow for 60 or 68 h. After the respective time, worms were transferred to the tubes, washed twice with M9 buffer, frozen in methanol for 1 h at -20 °C. After 1 h, worms were washed twice with M9 buffer and stained with 1 ng/mL DAPI for 10 min. After staining, worms were washed three times with M9 and transferred in to microscope slides. Worms were visualized by fluorescence microscopy. We scored the development stage of the worms using gonad structure.

Heat shock experiment

For reporter assay, synchronized first-day young adult worms grown at 20 ℃ were heat shocked at 35 ℃ for 1 h and left to recover for 4 h. Worms were observed using an RFP filter on a Leica MZ10 F fluorescence microscope for the expression of mCherry. For qPCR, synchronized first-day young adult worms (n=130-150) grown at 20 ℃ were heat shocked at 33 ℃ for 1 h. After heat shock worms were collected, washed three times with M9 and snap frozen at -80 ℃.

Salt induction experiment

For reporter assay, starved L1-stage worms were placed on NGM plates containing 52 mM and 150 mM NaCl. After 72 h worms were observed under a fluorescence microscope for the expression of GFP. For qPCR, starved L1-stage worms (n=130-150) were placed on NGM plates containing 52 mM and 150 mM NaCl. After 72 h worms were collected, washed three with M9 and snap frozen at -80 ℃.

RNAi Screening

Indicated RNAi clones were streaked on plates containing ampicillin (100 μg/mL) and tetracycline (100 μg/mL) and incubated overnight at 37 ℃. The overnight culture was inoculated in a 2ml LB with ampicillin (100 μg/mL) and incubated for 6-8 h at 37 ℃ in a shaking incubator. The grown bacterial culture was seeded on a dried NGM plate containing 1mM IPTG and 100 μg/mL ampicillin. Seeded plates were dried at room temperature then incubated for 24 h at 37 ℃. To all RNAi experiment except for hda-1, L1 worms were spotted

on RNAi plates, and their progeny(F1) were used for the experiments. For hda-1 RNAi, spotted L1 (P0) were used for all the experiments.

RNAi sensitivity assay

Three L3/L4 (P0) worms are transferred from OP50 seeded plates to EV, dpy-10, unc-15 and hmr-1 RNAi plates. Worms are left to grow for 48 hours before being transferred to fresh RNAi plates. After 24 hours the worms are transferred again to a fresh RNAi plate. Brood size is counted for each plate, and the sum is divided by three to give average brood size of the worm as a control. The severity of phenotype in dpy-10 RNAi was assessed by comparing the body length of mutant worms (F1) with wild-type (F1) in dpy-10 RNAi. For unc-15, a number of adult worms (F1) that are able to move their body are counted. For hmr-1, the percentage of dead eggs was measured.

Fertility assay of TSA treated worms

NGM plates containing 4 µM Trichostatin A (TSA) or Dimethyl sulfoxide (DMSO) were prepared. OP50 containing 4 µM TSA or DMSO was spotted on respective plates. L1(P0) worms were transferred into TSA or DMSO plates and incubated at 20 °C. Either ten L4 worms were picked and transferred to an individual plate, or 3 L4 worms per plate were picked in three TSA or DMSO plates. Fertility was assayed at 20 °C.

RNA extraction and qPCR

RNA was extracted using Direct-zol RNA miniprep. Extracted RNA was reverse transcribed to obtain cDNA using iScript cDNA synthesis kit (Bio-Rad). qPCR was performed with SYBR® Green (Biorad). Fold change in (C12C8.1, F44E5.4 and hsp-16.2) heat shock genes and gpdh-1(salt inducible gene) was measured using $2^{-\Delta\Delta Ct}$ formula. tba-1 and pmp-3 were used as a reference gene to calculate the fold change. Fold change was calculated by normalizing the heat shocked or salt treated worms to control untreated worms. Fold change of mutants relative to wild-type were presented on the graph. qRT-PCR was performed on three biological replicates.

Declarations:

Conflict of interest:

None.

Ethics approval and consent to participate:

Not applicable

Funding This project is funded by the University of Leeds. B.P. is supported by Leeds International Research Scholarship, and Y.C. is supported by the University Research Scholarship from the University of Leeds.

Acknowledgements

We thank James Cain for the technical support. We thank Dr Amit Kumar (Dr. Brockwell laboratory, University of Leeds) for help with western blot analysis, Laura Warwick and Dovile Milonaityte for carefully reading the manuscript.

Author's contribution:

B.P. designed and performed the majority of experiments. Y.C. performed RNAi sensitivity assay, and J.B. performed heat shock reporter assay. B.P. prepared the manuscript and all authors read and approved the final manuscript.

References

1. Tessarz, P. and T. Kouzarides, Histone core modifications regulating nucleosome structure and dynamics. Nature Reviews Molecular Cell Biology, 2014. **15**: p. 703.
2. Shilatifard, A., The COMPASS family of histone H3K4 methylases: mechanisms of regulation in development and disease pathogenesis. Annu Rev Biochem, 2012. **81**: p. 65-95.
3. Allis, C.D. and T. Jenuwein, The molecular hallmarks of epigenetic control. Nat Rev Genet, 2016. **17**(8): p. 487-500.
4. Celano, M., et al., Targeting post-translational histone modifications for the treatment of non-medullary thyroid cancer. Molecular and Cellular Endocrinology, 2018. **469**: p. 38-47.
5. Zhang, T., S. Cooper, and N. Brockdorff, The interplay of histone modifications - writers that read. EMBO Rep, 2015. **16**(11): p. 1467-81.
6. Berger, S.L., The complex language of chromatin regulation during transcription. Nature, 2007. **447**: p. 407.
7. Kouzarides, T., Chromatin Modifications and Their Function. Cell, 2007. **128**(4): p. 693-705.
8. Thakur, J.K., et al., A POLYCOMB group gene of rice (Oryza sativa L. subspecies indica), OsiEZ1, codes for a nuclear-localized protein expressed preferentially in young seedlings and during reproductive development. Gene, 2003. **314**: p. 1-13.
9. Wang, Y., et al., The Lysine Acetyltransferase GCN5 Is Required for iNKT Cell Development through EGR2 Acetylation. Cell Reports, 2017. **20**(3): p. 600-612.
10. Lau, A.C., et al., An H4K16 histone acetyltransferase mediates decondensation of the X chromosome in C. elegans males. Epigenetics & Chromatin, 2016. **9**: p. 44.
11. Barski, A., et al., High-resolution profiling of histone methylations in the human genome. Cell, 2007. **129**(4): p. 823-37.
12. Pokholok, D.K., et al., Genome-wide map of nucleosome acetylation and methylation in yeast. Cell, 2005. **122**(4): p. 517-27.
13. Pena, P.V., et al., Histone H3K4me3 binding is required for the DNA repair and apoptotic activities of ING1 tumor suppressor. J Mol Biol, 2008. **380**(2): p. 303-12.
14. Wysocka, J., et al., A PHD finger of NURF couples histone H3 lysine 4 trimethylation with chromatin remodelling. Nature, 2006. **442**: p. 86.
15. Ardehali, M.B., et al., Drosophila Set1 is the major histone H3 lysine 4 trimethyltransferase with role in transcription. EMBO J, 2011. **30**(14): p. 2817-28.
16. Howe, F.S., et al., Is H3K4me3 instructive for transcription activation? Bioessays, 2017. **39**(1): p. 1-12.
17. Margaritis, T., et al., Two distinct repressive mechanisms for histone 3 lysine 4 methylation through promoting 3'-end antisense transcription. PLoS Genet, 2012. **8**(9): p. e1002952.
18. Lorenz, D.R., et al., CENP-B cooperates with Set1 in bidirectional transcriptional silencing and genome organization of retrotransposons. Mol Cell Biol, 2012. **32**(20): p. 4215-25.
19. Robert, V.J., et al., The SET-2/SET1 histone H3K4 methyltransferase maintains pluripotency in the Caenorhabditis elegans germline. Cell Rep, 2014. **9**(2): p. 443-50.
20. Li, T. and W.G. Kelly, A role for Set1/MLL-related components in epigenetic regulation of the Caenorhabditis elegans germ line. PLoS Genet, 2011. **7**(3): p. e1001349.

21. Simonet, T., et al., Antagonistic functions of SET-2/SET1 and HPL/HP1 proteins in C. elegans development. Dev Biol, 2007. **312**(1): p. 367-83.
22. Krogan, N.J., et al., COMPASS, a histone H3 (Lysine 4) methyltransferase required for telomeric silencing of gene expression. J Biol Chem, 2002. **277**(13): p. 10753-5.
23. Lee, J.H. and D.G. Skalnik, CpG-binding protein (CXXC finger protein 1) is a component of the mammalian Set1 histone H3-Lys4 methyltransferase complex, the analogue of the yeast Set1/COMPASS complex. J Biol Chem, 2005. **280**(50): p. 41725-31.
24. Skalnik, D.G., The epigenetic regulator Cfp1. Biomol Concepts, 2010. **1**(5-6): p. 325-34.
25. Clouaire, T., S. Webb, and A. Bird, Cfp1 is required for gene expression-dependent H3K4 trimethylation and H3K9 acetylation in embryonic stem cells. Genome Biol, 2014. **15**(9): p. 451.
26. Chun, K.T., et al., The epigenetic regulator CXXC finger protein 1 is essential for murine hematopoiesis. PLoS One, 2014. **9**(12): p. e113745.
27. Chen, R.A., et al., Extreme HOT regions are CpG-dense promoters in C. elegans and humans. Genome Res, 2014. **24**(7): p. 1138-46.
28. Thomson, J.P., et al., CpG islands influence chromatin structure via the CpG-binding protein Cfp1. Nature, 2010. **464**(7291): p. 1082-6.
29. Clouaire, T., et al., Cfp1 integrates both CpG content and gene activity for accurate H3K4me3 deposition in embryonic stem cells. Genes Dev, 2012. **26**(15): p. 1714-28.
30. Tate, C.M., J.H. Lee, and D.G. Skalnik, CXXC finger protein 1 restricts the Setd1A histone H3K4 methyltransferase complex to euchromatin. FEBS J, 2010. **277**(1): p. 210-23.
31. Mahadevan, J. and D.G. Skalnik, Efficient differentiation of murine embryonic stem cells requires the binding of CXXC finger protein 1 to DNA or methylated histone H3-Lys4. Gene, 2016. **594**(1): p. 1-9.
32. Miller, T., et al., COMPASS: a complex of proteins associated with a trithorax-related SET domain protein. Proc Natl Acad Sci U S A, 2001. **98**(23): p. 12902-7.
33. Lee, J.H., et al., Identification and characterization of the human Set1B histone H3-Lys4 methyltransferase complex. J Biol Chem, 2007. **282**(18): p. 13419-28.
34. Brown, D.A., et al., The SET1 Complex Selects Actively Transcribed Target Genes via Multivalent Interaction with CpG Island Chromatin. Cell Rep, 2017. **20**(10): p. 2313-2327.
35. Xiao, Y., et al., Caenorhabditis elegans chromatin-associated proteins SET-2 and ASH-2 are differentially required for histone H3 Lys 4 methylation in embryos and adult germ cells. Proc Natl Acad Sci U S A, 2011. **108**(20): p. 8305-10.
36. Lamitina, T., C.G. Huang, and K. Strange, Genome-wide RNAi screening identifies protein damage as a regulator of osmoprotective gene expression. Proc Natl Acad Sci U S A, 2006. **103**(32): p. 12173-8.
37. van Oosten-Hawle, P., R.S. Porter, and R.I. Morimoto, Regulation of organismal proteostasis by trans-cellular chaperone signaling. Cell, 2013. **153**(6): p. 1366-1378.
38. Prahlad, V., T. Cornelius, and R.I. Morimoto, Regulation of the cellular heat shock response in Caenorhabditis elegans by thermosensory neurons. Science, 2008. **320**(5877): p. 811-4.
39. Snutch, T.P., M.F. Heschl, and D.L. Baillie, The Caenorhabditis elegans hsp70 gene family: a molecular genetic characterization. Gene, 1988. **64**(2): p. 241-55.
40. Jones, D., et al., Structure, expression, and evolution of a heat shock gene locus in Caenorhabditis elegans that is flanked by repetitive elements. J Biol Chem, 1986. **261**(26): p. 12006-15.

41. Tang, Z., et al., SET1 and p300 Act Synergistically, through Coupled Histone Modifications, in Transcriptional Activation by p53. Cell. **154**(2): p. 297-310.
42. Tie, F., et al., CBP-mediated acetylation of histone H3 lysine 27 antagonizes Drosophila Polycomb silencing. Development, 2009. **136**(18): p. 3131-41.
43. Zhao, X., et al., Crosstalk between NSL histone acetyltransferase and MLL/SET complexes: NSL complex functions in promoting histone H3K4 di-methylation activity by MLL/SET complexes. PLoS Genet, 2013. **9**(11): p. e1003940.
44. Eastburn, D.J. and M. Han, A gain-of-function allele of cbp-1, the Caenorhabditis elegans ortholog of the mammalian CBP/p300 gene, causes an increase in histone acetyltransferase activity and antagonism of activated Ras. Molecular and Cellular Biology, 2005. **25**(21): p. 9427-9434.
45. Shi, Y. and C. Mello, A CBP/p300 homolog specifies multiple differentiation pathways *in Caenorhabditis elegans.* Genes & Development, 1998. **12**(7): p. 943-955.
46. Solari, F. and J. Ahringer, NURD-complex genes antagonise Ras-induced vulval development in Caenorhabditis elegans. Curr Biol, 2000. **10**(4): p. 223-6.
47. Choy, S.W., et al., C. elegans SIN-3 and its associated HDAC corepressor complex act as mediators of male sensory ray development. Biochem Biophys Res Commun, 2007. **358**(3): p. 802-7.
48. Bender, A.M., et al., lin-35/Rb and the CoREST ortholog spr-1 coordinately regulate vulval morphogenesis and gonad development in C. elegans. Dev Biol, 2007. **302**(2): p. 448-62.
49. Gregoretti, I.V., Y.M. Lee, and H.V. Goodson, Molecular evolution of the histone deacetylase family: functional implications of phylogenetic analysis. J Mol Biol, 2004. **338**(1): p. 17-31.
50. Grzenda, A., et al., Sin3: master scaffold and transcriptional corepressor. Biochim Biophys Acta, 2009. **1789**(6-8): p. 443-50.
51. Meier, K. and A. Brehm, Chromatin regulation: How complex does it get? Epigenetics, 2014. **9**(11): p. 1485-1495.
52. Hayakawa, T. and J. Nakayama, Physiological roles of class I HDAC complex and histone demethylase. J Biomed Biotechnol, 2011. **2011**: p. 129383.
53. Basta, J. and M. Rauchman, The nucleosome remodeling and deacetylase complex in development and disease. Transl Res, 2015. **165**(1): p. 36-47.
54. Passannante, M., et al., Different Mi-2 Complexes for Various Developmental Functions in Caenorhabditis elegans. Plos One, 2010. **5**(10).
55. De Vaux, V., et al., The Caenorhabditis elegans LET-418/Mi2 plays a conserved role in lifespan regulation. Aging Cell, 2013. **12**(6): p. 1012-1020.
56. Ahringer, J. and S.M. Gasser, Repressive Chromatin in Caenorhabditis elegans: Establishment, Composition, and Function. Genetics, 2018. **208**(2): p. 491-511.
57. Kaser-Pebernard, S., F. Muller, and C. Wicky, LET-418/Mi2 and SPR-5/LSD1 cooperatively prevent somatic reprogramming of C. elegans germline stem cells. Stem Cell Reports, 2014. **2**(4): p. 547-59.
58. De Vaux, V., et al., The Caenorhabditis elegans LET-418/Mi2 plays a conserved role in lifespan regulation. Aging Cell, 2013. **12**(6): p. 1012-20.
59. von Zelewsky, T., et al., The C. elegans Mi-2 chromatin-remodelling proteins function in vulval cell fate determination. Development, 2000. **127**(24): p. 5277-84.
60. Crump, N.T., et al., Dynamic acetylation of all lysine-4 trimethylated histone H3 is evolutionarily conserved and mediated by p300/CBP. Proc Natl Acad Sci U S A, 2011. **108**(19): p. 7814-9.
61. Vastenhouw, N.L., et al., Gene expression: long-term gene silencing by RNAi. Nature, 2006. **442**(7105): p. 882.

62. Zhou, B.O. and J.-Q. Zhou, Recent Transcription-induced Histone H3 Lysine 4 (H3K4) Methylation Inhibits Gene Reactivation. The Journal of Biological Chemistry, 2011. **286**(40): p. 34770-34776.
63. O'Brien, T. and J.T. Lis, RNA polymerase II pauses at the 5' end of the transcriptionally induced Drosophila hsp70 gene. Mol Cell Biol, 1991. **11**(10): p. 5285-90.
64. Cui, M., E.B. Kim, and M. Han, Diverse chromatin remodeling genes antagonize the Rb-involved SynMuv pathways in C. elegans. PLoS Genet, 2006. **2**(5): p. e74.
65. Beurton, F., et al., Physical and functional interaction between SET1/COMPASS complex component CFP-1 and a Sin3 HDAC complex. bioRxiv, 2018: p. 436147.
66. Adam, C., et al., The PHD finger protein Spp1 has distinct functions in the Set1 and the meiotic DSB formation complexes. PLOS Genetics, 2018. **14**(2): p. e1007223.

Figures legends

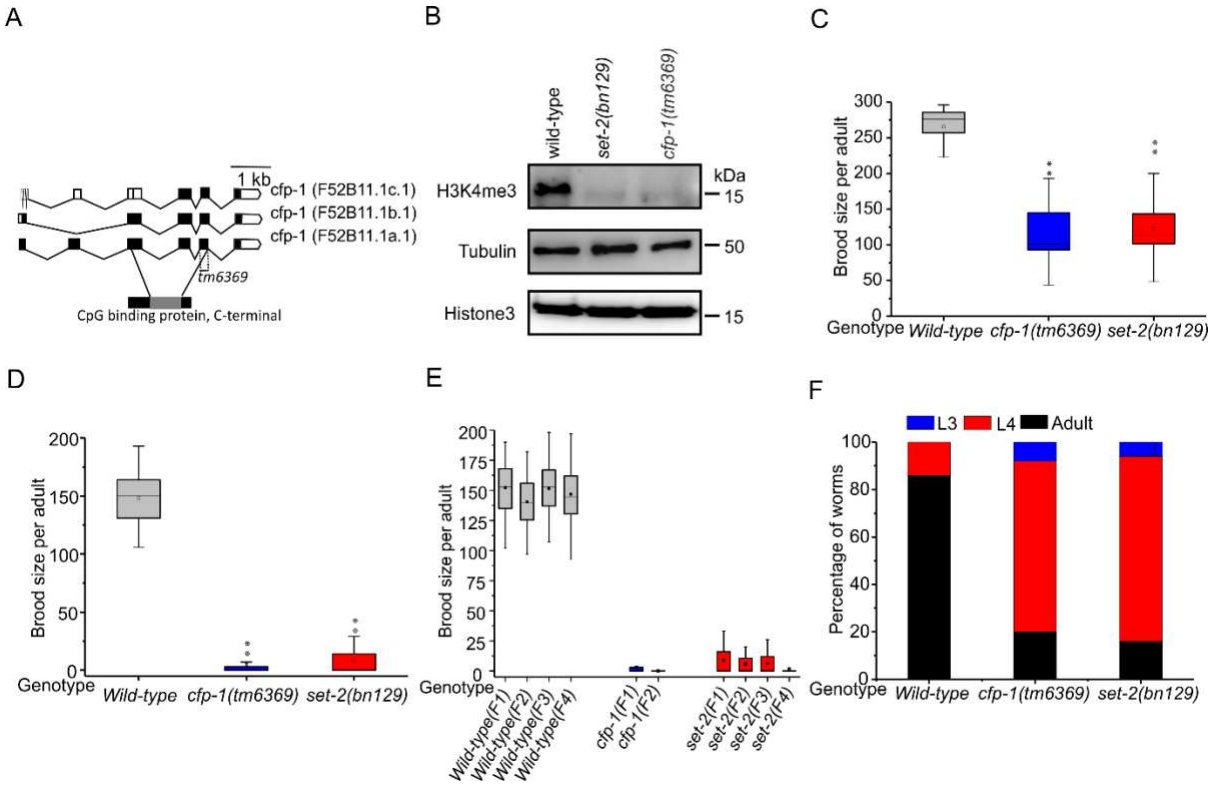

Figure. 1 cfp-1(tm6369) is a loss of function allele. (A) Diagrammatic representation of the cfp-1(tm6369) allele. 254 bp encompassing exon 5 (F52B11.1a.1) and part of the intron upstream and downstream region is deleted. The deleted region is indicated by the dashed line. Black colour denotes the exon and grey colour denotes the CpG binding domain. (B) Western blot analysis showing the reduced level of H3K4me3 in cfp-1(tm6369) and set-2(bn129) mutants compared to wild type. Histone 3 (H3) and tubulin were used as a loading control. This figure is representative of one biological replicate. (C and D) Total brood size assay for wild-type (grey), cfp-1(tm6369) (blue) and set-2(bn129) (red) mutants. (C) The average brood size of cfp-1(tm6369) and set-2(bn129) mutants was significantly reduced compared to wild-type at 20 °C. For the figure, two biological replicates were combined (n=10 in each replicate). (D) Fertility was severely compromised at 25 °C, and 70% of cfp-1(tm6369) and set-2(bn129) mutants were sterile. For the figure, two biological replicates were combined (n=10 in each replicate). (E) Mortal germline phenotype assay of cfp-1(tm6369) and set-2(bn129) mutants. cfp-1(tm6369) mutant was completely sterile at F2 generation. For the figure, two biological replicates were combined (n=10 in each replicate).

(F) Developmental progress of cfp-1(tm6369), set-2(bn129) and wild-type embryos monitored after 60 h at 20 ℃. cfp-1(tm6369) and set-2(bn129) mutants displayed stochastic delays in development from an embryo into a young adult. The figure is average of two independent experiments (n > 30 per strain in each experiment. Combined number of animals from two replicates: WT(172), cfp-1(tm6369) (101), set-2(bn129) (137)). P-values were calculated using the student t-test: ** = P<0.01.

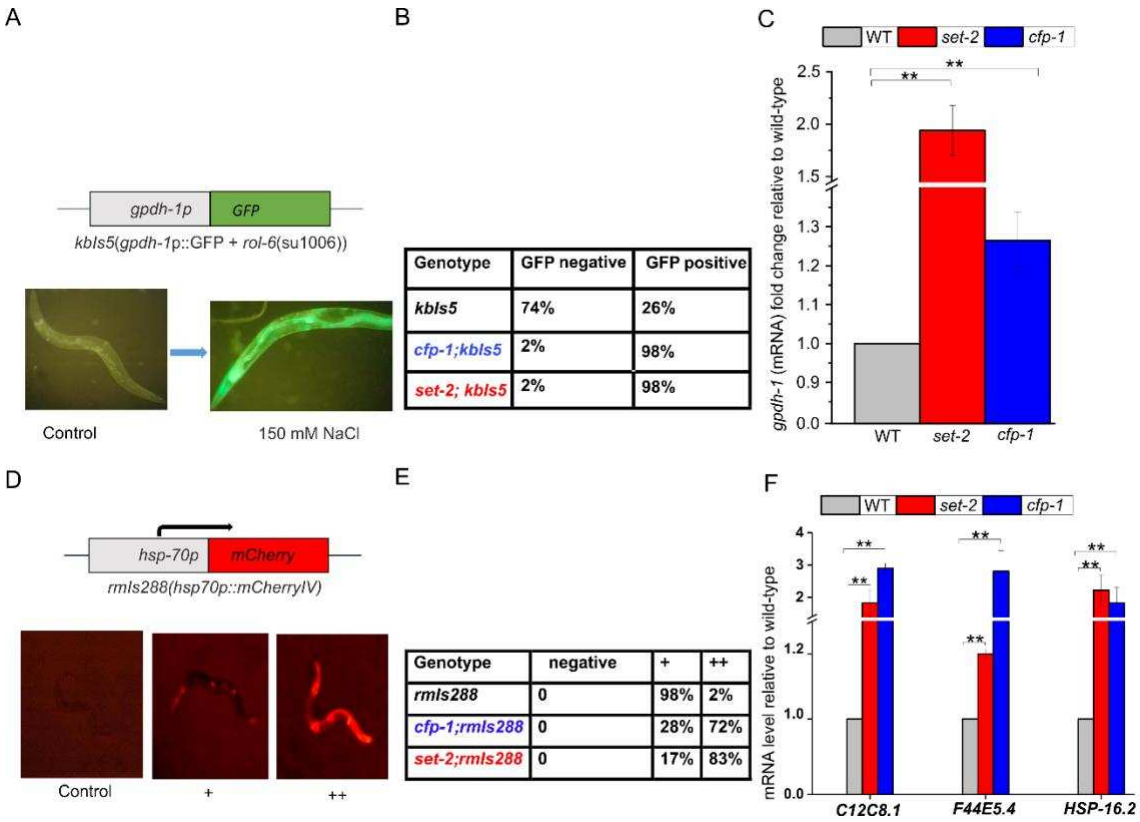

Genotype	GFP negative	GFP positive
kbIs5	74%	26%
cfp-1;kbIs5	2%	98%
set-2; kbIs5	2%	98%

Genotype	negative	+	++
rmIs288	0	98%	2%
cfp-1;rmIs288	0	28%	72%
set-2;rmIs288	0	17%	83%

Figure 2. Loss of cfp-1 or set-2 results in stronger expression of inducible genes. (A) The VP198 (gpdh-1p::GFP) strain contains GFP downstream of a gpdh-1 promoter which is expressed in worms when shifted to a higher concentration of salt (150 mM). (B) Table showing the percentage of GFP positive and negative worms. L1 worms were grown at hypertonic conditiosn (150 mM) for 72 h. Higher percentage of COMPASS mutants show stronger GFP induction compared to kbls5 in a wild-type background. This experiment has been repeated, and similar result was observed (n>30 per strain in each replicate). (C) qPCR of the gpdh-1 transcript at hypertonic condition (150 mM) in wild-type (grey), cfp-1(tm6369) (blue) and set-2(bn129) (red) mutants. gpdh-1 expression level is higher in cfp-1(tm6369) and set-2(bn129) mutants relative to wild-type treated to higher salt concentration. pmp-3 and tba-1 genes were used for normalisation. The figure is average of 3 biological replicates (n=130-

150 in each replicate). (D) The AM722 (hsp70p::mCherry) strain contains an mCherry reporter gene downstream of an hsp-70 promoter which is expressed during heat shock. (+) moderate expression, (++) stronger expression of mCherry. (E) Table showing the percentage of worms expressing mCherry. Worms were heat shocked at 35 °C for 1 h and left them to recover for 4 h. COMPASS mutants show stronger mCherry induction compared to rmls288. This experiment has been repeated, and similar result was observed (n>25 per strain in each replicate). (F) qPCR of transcript of heat shock genes C12C8.1, F44E5.4 and hsp-16.2 in wild-type (grey), cfp-1(tm6369) (blue) and set-2(bn129) (red) mutants before and after heat shock at 33°C for 1 h. C12C8.1, F44E5.4 and hsp-16.2 relative transcript levels are higher in cfp-1(tm6369) and set-2(bn129) mutants compared wild-type heat shocked animals. pmp-3 and tba-1 genes were used for normalisation. The figure is average of 3 biological replicates (n=130-150 in each replicate). For figures C and F, statistics were done in delta Ct values. P-values were calculated using the student t-test: **= P<0.01. Error bars represent ± standard error of the mean (SEM).

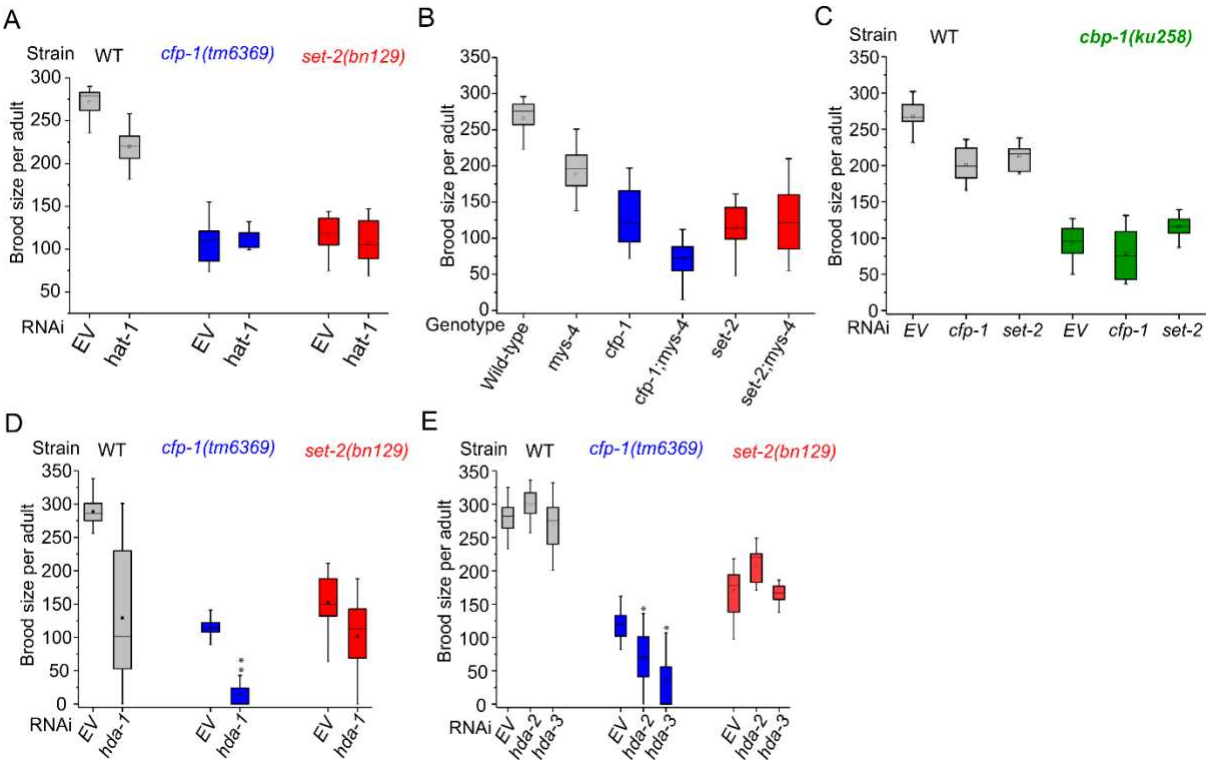

751

752 **Figure 3**: **cfp-1 genetically interacts with class I HDAC but not with HATs to regulate**
753 **fertility.** (A-C) Brood size assays showing no genetic interactions between cfp-1 and HATs
754 using RNAi knockdown. A multiplicative method was used to identify whether two genes
755 interact to regulate fertility or not. (A) Brood size of wild-type (WT) (grey), cfp-1(tm6369)
756 (blue) and set-2(bn129) (red) mutants upon hat-1 RNAi. For control, worms were fed on
757 HT115 E. coli strain that has empty RNAi feeding vector (EV). RNAi knockdown of hat-1 did
758 not have a significant impact on the brood size of cfp-1(tm6369) or set-2(bn129) mutants, as
759 compared to the EV RNAi controls. Two replicates were combined for the figure (n=15 in each
760 replicate). (B) Brood sizes of wild-type (grey), mys-4(tm3161) (grey), cfp-1(tm6369) (blue),
761 set-2(bn129) (red), cfp-1(tm6369);mys-4(tm3161) (blue) and set-2(bn129);mys-4(tm3161)
762 (red) mutants at 20 °C. The average brood size of cfp-1(tm6369);mys-4(tm3161) double mutant
763 was reduced brood size compared to the single mutants. However, the difference in brood size
764 is not synergistic (based on the Null hypothesis T-test). Two replicates were combined for the
765 figure (n=10 in each replicate). (C) Brood sizes of WT (grey) and cbp-1(ku258) (green) mutant

upon RNAi of EV, cfp-1 and set-2. Brood sizes of cbp-1(ku258) on RNAi of cfp-1 or set-2 was similar to EV. Two replicates were combined (n=9-10 in each replicate). (D and E) Brood size assays showing genetic interactions between cfp-1 and class I HDACs using RNAi knockdown. (D) Average brood size of wild-type (grey), cfp-1(tm6369) (blue) and set-2(bn129) (red) mutants upon hda-1 RNAi. hda-1 RNAi resulted in a higher percentage of embryonic lethality at F1, so fertility was assayed at P0. RNAi knockdown of hda-1 resulted in a reduction in brood size in both wild-type and cfp-1(tm6369) and set-2(bn129) mutants. Null hypothesis t-test (refer to the methods section) showed a synergistic interaction between hda-1 and cfp-1 but not set-2. Three biological replicates were combined the figure (n=10 in each replicate). (E) The average brood size on RNAi knockdown of hda-2 or hda-3 in wild-type (grey), cfp-1(tm6369) (blue) and set-2(bn129) (red) mutants. Brood size of cfp-1(tm6369) mutants was further reduced in these RNAi but had no significant impact on the brood size of set-2(bn129) mutant. Three biological replicates were combined for the figure (n=10-15 in each replicate)

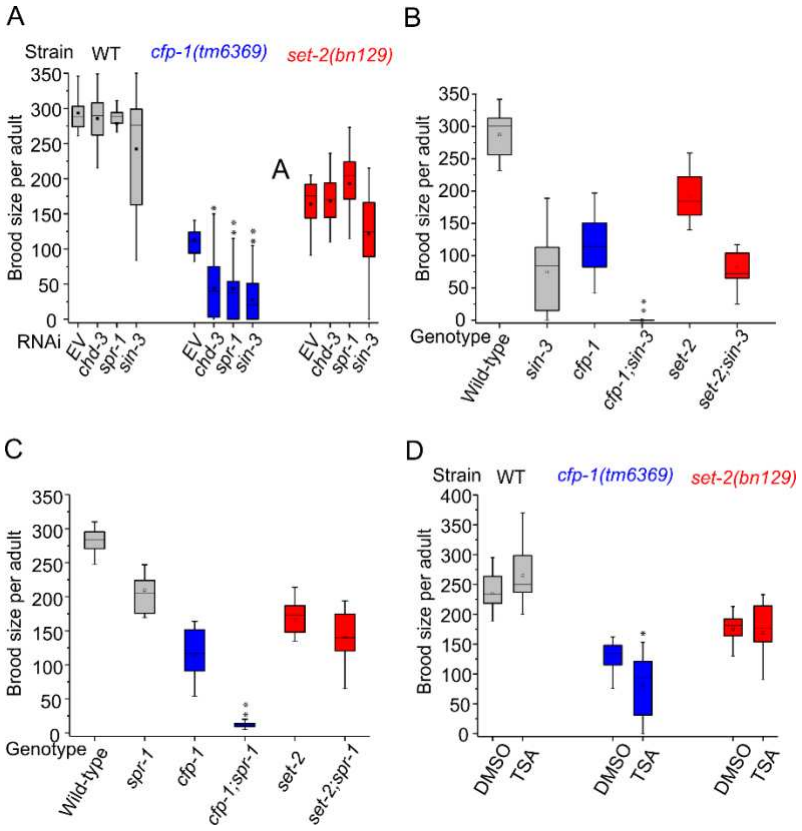

781

782 **Figure 4. Synergistic interaction between CFP-1 and HDAC1/2 complexes**

783 Brood size assays showing genetic interactions between cfp-1 and class 1/2 HDACs using
784 RNAi knockdown (A), double mutants (B and C) and HDACs inhibitor (D). A multiplicative
785 method was used to identify whether two genes interact to regulate fertility or not. For control,
786 worms are fed on HT115 E. coli strain that has empty RNAi feeding vector (EV). (A) Average
787 brood sizes of wild-type (grey), cfp-1(tm6369) (blue) and set-2(bn129) (red) mutants upon
788 RNAi of sin-3 or spr-1 or chd-3. Brood size of cfp-1(tm6369) mutants was further reduced in
789 these RNAi but had no significant impact on the brood size of set-2(bn129) mutant. Three
790 biological replicates were combined for the figure (n=10-15 in each replicate) (B) Average
791 brood size of sin-3(tm1276) mutants. cfp-1(tm6369);sin-3(tm1276) (blue) double mutant was
792 sterile. Brood size of set-2(bn129);sin-3(tm1276) (red) was similar to the brood size of sin-
793 3(tm1276) (grey) showing no genetic interaction. Two biological replicates were combined for
794 the figure (n=10 in each replicate). (C) Average brood size of spr-1(ok2144) mutants. Average

brood size of cfp-1(tm6369);spr-1(ok2144) (blue) mutant was significantly lower compared to single mutants, whereas the brood size of set-2(bn129);spr-1(ok2144) (red) mutant was similar to set-2(bn129) (red) mutant. Two biological replicates were combined for the figure (n=10 in each replicate). (D) Brood size of wild-type (grey), cfp-1(tm6369) (blue) and set-2(bn129) (red) mutants treated with control (DMSO) or Trichostatin A (TSA). Average brood size of cfp-1(tm6369) mutant was slightly but significantly reduced when treated with TSA. Three biological replicates were combined for the figure (n=9-10 in each replicate). P-values were calculated using the one-tailed student t-test: ** = $P<0.01$, * = $P<0.05$.

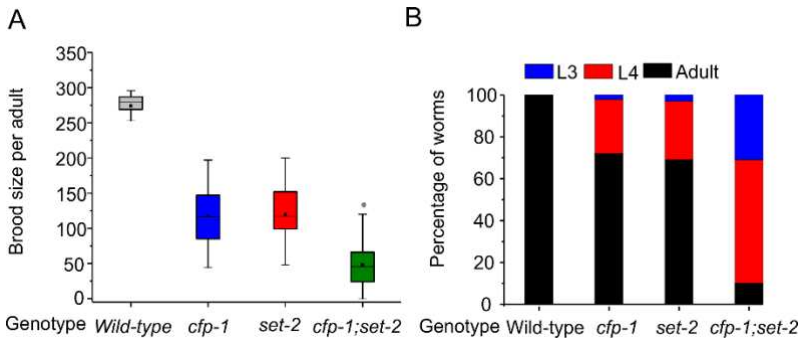

Figure 5: **cfp-1 and set-2 independently regulate fertility and growth**. (**A**) Brood size of wild-type (grey), cfp-1(tm6369) (blue), set-2(bn129) (red) and cfp-1(tm6369);set-2(bn129) (green) mutants at 20 °C. The average brood size of cfp-1(tm6369);set-2(bn129) double mutant was significantly reduced compared to single mutants, however the difference in brood size is not synergistic (based on Null hypothesis T-test). Three biological replicates were combined for the figure (n=10 in each replicate). P-values were calculated using one-tailed student t-test: * = P<0.05. (B) Developmental progress of wild-type, cfp-1(tm6369), set-2(bn129) and cfp-1(tm6369);set-2(bn129) embryo monitored at 68 h at 20 °C. cfp-1(tm6369);set-2(bn129) mutants grow slower than cfp-1(tm6369) and set-2(bn129) single mutants. The figure is average of two independent experiments (n>30 per strain in each experiment. Combined number of animals from two replicates: WT (129), cfp-1(tm6369) (73), set-2(bn129) (103) and cfp-1(tm6369);set-2(bn129) (171)).

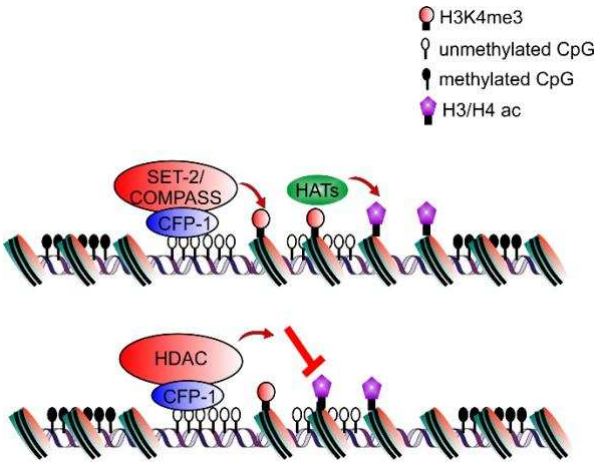

Figure 6: **Proposed model indicating that CFP-1 cooperates with SET-2/COMPASS and/or with HDACs in a context-dependent manner**. Canonical function of CFP-1 is to recruit SET-2/COMPASS complex at promoter regions by binding into unmethylated CpG island. The non-canonical function of CFP-1: CFP-1 could also recruit HDAC complexes at promoter region to deacetylate the histones. Based on the physiological condition CFP-1 could either interact with the COMPASS complex or with HDAC complexes.

830